Exploiting the "survival of the likeliest" to enable evolution-guided drug design

Chuan Liu[1,2,*], Scott M. Leighow[1,*], Haider Inam[1], Boyang Zhao[1], and Justin R. Pritchard[1,3,‡*]

1. The Pennsylvania State University, Department of Biomedical Engineering, University Park PA, 16802.
2. Department of Oncology, Shanghai General Hospital, Shanghai Jiao Tong University School of Medicine, Shanghai, 200080, China
3. The Huck Institute for the Life Sciences, Center for the Evolution of Resistance, The Pennsylvania State University

‡. To whom correspondence should be addressed: jrp94@psu.edu

***. These authors contributed equally**

Running Title: Survival of the likeliest guides drug design

Summary

Theoretical treatments of evolutionary dynamics tend to model the probability that a single "resistant" species will arise in a population. However, experimental studies have identified a diversity of mutations that can lead to genetic resistance. By quantitatively predicting mutations that occur across an entire drug target during treatment, we identify and bridge a fundamental gap in drug resistance theory: that nucleotide/codon substitution biases can dictate which resistant variants arise in the clinic. We find that the likeliest mutation can beat the most resistant mutation. This creates a new paradigm in drug resistance that we term *"survival of the likeliest"*. We use epidemiological evidence in leukemia, isogenic experiments, stochastic dynamics, and large-scale simulations to support this theory. In addition, this work has strong implications for drug design because not all resistance liabilities are created equal. In pathogenic populations that exhibit survival of the likeliest, exploiting the least likely evolutionary path can minimize resistance across a population during widespread drug use, even when a vulnerability-free molecule or combination cannot be made.

Correspondence to:
Justin Pritchard
211 Wartik Lab
The Pennsylvania State University
University Park, PA 16802
Jrp94@psu.edu

Data and Code Availability
https://github.com/pritchardlabatpsu/SurvivalOfTheLikeliest/

Introduction

Over the last 150 years, the most powerful demonstration of natural selection is the pervasiveness of genetic resistance following the adoption of new drugs for viruses, prokaryotes, eukaryotes, and cancers[1–7]. There are two scales that determine which variants arise: the host-level variables affecting *de novo* resistance generation and the community level variables affecting the global spread of resistance. The *de novo* variables include growth rates in the presence and absence of drug (which are often measured) as well as mutation rate, codon structure, genetic context and pharmacology (which are seldom measured). Importantly, human cancers offer a unique opportunity to investigate the process of parallel *de novo* resistance evolution in individual hosts because they lack community level variables that can spread variants across a population (Figure 1A).

In examining the theory surrounding *de novo* drug resistance evolution, foundational stochastic models of evolutionary dynamics have stressed the strong probability that drug resistance mutations pre-occur in large tumors[1,8–12]. Resistance probabilities for some processes can be calculated analytically[1,10,13], and have been used to offer important principles of successful combination therapy[10]. Moreover, deeper measurements of tumor heterogeneity have measured levels of genetic diversity that are consistent with theory[14]. Experimental studies of genetic drug resistance typically examine the identity and number of the individual resistant mutations that are identified in patients. Then, they test the amount of drug resistance conferred in an experimental system[15–17]. But the fact that multiple resistance mutations have been detected and validated across patients with a given disease suggests that it is not only the single fittest mutation that grows out. Thus, a fundamental gap in our theoretical understanding of resistance evolution keeps us from rationalizing the molecular diversity that is observed in the clinic.

This gap in theory also creates a gap in patient care. In the targeted therapy of cancer, as first-generation drugs are used and resistance liabilities are identified, drug discovery scientists have raced to develop second-generation drugs that can target resistance mutations[18–21]. Second-generation inhibitors can improve clinical outcomes in drug resistant and drug naïve patients, but vulnerabilities persist because unmet need drives rapid drug development in the face of immature patient data[18,20,21]. Thus, molecular design occurs before we know the true prevalence of a specific mutation in the population. Structure-based drug design is now the industry standard to create potent second-generation inhibitors and has succeeded in ABL1+ leukemias[19,22], c-KIT/PDGFR mutated GIST[23], ALK/EGFR+ lung cancers[24,25], and TRK fusions[26]. But rational design is based upon the biophysics of binding and not evolution. Thus, it can often identify whether a mutation can cause resistance, but it can't determine how often we would expect to see that mutation in the clinic[27]. Using evolutionary theory to prospectively identify which mutations (and with what frequency) occur after real-world drug use will improve pharmaceutical design by developing a broader picture of drug resistance evolution before clinical data has matured and the true population incidences are known.

In this study, we observed that in the 17-year parallel evolution experiment of global imatinib treatment for chronic myelogenous leukemia (CML), the substitution probability of a mutation in BCR-ABL is more significant in shaping the real-world incidence of resistance mutations than the degree of resistance conferred by the mutation. We found that the survival of the "fittest", or most drug resistant, allele can be beaten in the real world by the survival of the "likeliest" allele. We also reformulated and expanded a clinically parameterized stem cell model of imatinib treatment as a multi-mutation stochastic process. Then we used parameters that were fixed from *in vitro* experiments to demonstrate that we can *a priori* predict the distribution of real-world mutations from a mechanistic model and *in vitro* data. This model can forecast the global abundance of specific amino acid mutations from first principles evolutionary mechanisms

(without fitting to prevalence data) with surprising accuracy (Spearman correlation 0.78). Using our evolutionary model to examine current second-generation inhibitors as well as hypothetical drugs, we show that an evolutionarily-enabled approach to structure-based drug design could prioritize the most likely mutants to grow out in a population, and not just potency as measured by changes in free energy. Using evolution to guide drug design can allow one to select the evolutionarily optimal mutation when forced to choose between similar thermodynamic or phenotypic outcomes.

Results

A single salt bridge in ABL1 suggests that clinical abundance may not be predicted by the amount of drug resistance conferred.

We first examined two drug resistance mutations identified in the literature that exist at the same amino acid in the BCR-ABL oncogene: E255. E255 forms a salt bridge interaction with K247, stabilizing the phosphate binding loop (P-loop) that clamps over the ATP competitive inhibitor in the active site of the molecule (Figure 1B). E255 can mutate to become either E255V or K, both of which abolish the charge interaction and promote imatinib resistance (Figure 1C). Interestingly, tallying the abundance of E255V and E255K mutations across clinical studies suggested that E255K was more prevalent (21 patients) than E255V (10 patients) ($p<0.05$, chi-square test).

Next we sought to examine why E255K might be more prevalent than E255V. We made BaF3 cells that harbored wild type, E255V and E255K BCR-ABL (a common model for BCR-ABL targeted therapies), and we examined their relative sensitivity to imatinib. As expected, both mutations provided resistance to imatinib, but E255K provided significantly less resistance to imatinib than E255V (Figure 1D). While further investigation into the biophysics of P-loop dynamics could reveal the molecular mechanism behind this difference in drug resistance, we aimed to explore how a mutation that is worse at conferring drug resistance (regardless of the biophysical mechanisms) might become more prevalent in humans. Because the less drug resistant variant appeared to grow out more often, we examined the relative growth rate of E255V and K in the absence of drug. If E255V grows significantly slower before imatinib exposure, that might help to explain its lower incidence in a human population. However, the relative growth rates for E255V, E255K and wild type BCR-ABL cells were indistinguishable (Figure 1E).

Thus, we hypothesized that a mutation from E>K might be more likely to occur than a mutation from E>V. Examining the genetic code, E>K requires a transition from G>A, while mutating from E>V requires a transversion from A>T. No other single nucleotide substitutions can cause these two mutations. While transitions are usually more likely than transversions, we sought a direct measurement of the mutation bias in ABL1. To do this, we turned to the Broad ExAC data (see Methods, Supplemental Table 1) to estimate ABL1 mutation bias. Using this data set we identified 224 synonymous mutations in the ABL1 gene (Figure 1F). Splitting these mutations by nucleotide type on the transcribed strand to account for biases due to transcription coupled repair, we quantified the nucleotide substitution biases in the ABL1 gene. The measured bias was consistent with a classic transition-transversion bias, i.e. G>A mutations were much more likely than A>T mutations (34 times more frequently observed), supporting the hypothesis that E255K mutations are more probable than E255V mutations.

An analytical model of stochastic dynamics identifies parameter regimes in which survival of the likeliest can occur.

Because E255K was more likely to occur than E255V but not more fit in the presence or absence of drug treatment, we asked whether it makes theoretical sense that a more likely mutation can beat a more resistant one to create *de novo* drug resistance. To do this we developed a probability model for the stochastic evolutionary dynamics of a hypothetical drug target with two possible resistance alleles. Allele A is more resistant (more fit in the presence of drug) but less likely; Allele B is less resistant but more likely. The probability that either allele drives relapse was calculated from the allele-specific probabilities of seeding a detectable resistance clone. In cases where both resistance clones of both alleles are present, the first allele to reach clinical detection was considered to dominate relapse. This "race" to detection was formulated as two steps: mutation and growth. While Allele A is expected to grow out faster, Allele B is expected to mutate first, giving it a head start (Figure 2B). From this model, we derived an asymptotic solution for the probability that either allele drives relapse (Supplemental Appendix 1).

We then evaluated these probabilities across a region of the effective population size/mutation rate parameter space to identify parameter regimes where Allele B (the less fit, more likely allele) is more likely to drive relapse. This phenomenon of "survival of the likeliest" is strongest in the region of the phase plane with low mutation rates and a small effective population (Figure 2C), corresponding to populations with low heterogeneity. In low heterogeneity circumstances where the opportunity for mutation is limited, unlikely mutants may not spawn at all, regardless of the degree of fitness. Thus, under these conditions, it is more important for a resistance mutant to be likely than to be fit. However, as mutation rate and effective population size increase, Allele A is more likely to dominate, reflecting the classic "survival of the fittest" model of natural selection. Thus, the degree of heterogeneity, as shaped by population size and mutation rate, determines when substitution bias can play a driving role in drug resistance evolution.

These theoretical results point towards the apparent significance of mutation probability observed in real-world CML resistance incidence. The population structure of CML includes a well-characterized leukemic stem cell population of 10^5-10^6 cells that give rise to peripheral differentiated leukemic cells (Figure 2D). This hierarchy effectively restricts the population size, since only resistance mutations that occur in leukemic stem cells have any clinical consequence. Thus, CML can be placed in the "low heterogeneity" regime of the parameter space. Together, theory and empirical data support the principle that low heterogeneity populations are most strongly influenced by "survival of the likeliest."

Epidemiologic incidences of ABL1 resistance mutations are best predicted by how likely they are.

To approach this problem more comprehensively, we gathered data from hundreds of parallel clinical evolution experiments in BCR-ABL+ leukemias across four continents over 17 years (Supplemental Data 1)[28–33]. Specifically, we identified clinical trials with clear clinical resistance criteria and codon level resolution. 268 high confidence clinical cases of resistance were identified in these studies. Tallying mutations at individual amino acid positions, we found that the top 19 amino acid mutations account for ~95% of the resistance mutations identified (Figure 3A). Notably, 85% of the resistance prevalence captured by this set of mutations is caused by a mutation other than the fittest (T315I; imatinib IC_{50} 8711 nM). We generated three independent isogenic BaF3 cell lines for each of these 19 amino acids and measured the IC_{50} of imatinib in each cell line in triplicate across 11 serial drug dilutions (Figure 3B). While this set of 19 clinical point mutations in ABL1 is the most systematically assembled *in vitro* data set to date (regarding clinical abundance), many of these mutations have had their IC_{50}s measured in other resistance

studies in other labs. Thus, the literature presents us with an opportunity to estimate how genetic context and experimental conditions might affect drug response. Supplemental Figure 1 shows that cross study correlations are high (Pearson's rho~0.9 or higher for four studies), but systematic shifts in slope exist between studies. Systematic shifts across studies might suggest that the genetic drift in cell lines in an individual lab can influence drug potency and is consistent with recent findings[34]. Thus, we have an opportunity to account for the effects of genetic background upon drug resistance. To do this, we normalized all systematic differences between the data sets into one "mean" data set and combined all the data from the literature with our data (see Methods and Supplemental Data 1). This cross-study approach leverages the genetic drift across cell lines to get the best estimate of the average isogenic effect of BCR-ABL mutations.

Beyond IC_{50} measurements normalized for genetic background, we also measured the drug-free growth rates of all ABL1 mutants from 6-10 independent infections (Supplemental Figure 2A). Many independent infections were critical because individual clonal selections have a high variance. For each amino acid substitution, we also calculated the mutational probability given a resistance mutation event occurs (Figure 3D, see Methods, GitHub repository). Negative binomial regression was used (Supplemental Figure 2B, R-markdown file on GitHub) to predict the incidence of individual resistance mutants across the human population. After considering all possible single variable models, we built multivariate models by identifying the best N-variable model by leave-one-out-cross validation (LOOCV) (Supplemental Figure 2C). A two-variable model that contained normalized IC_{50} values across 19 isogenic mutant cell lines and the substitution biases in individual codons within the drug target was well supported by the data (Figure 3E). While the statistical model suggested that the amount of drug resistance and the substitution bias were both significant and predictive (Figure 3E and Supplemental Figure 2, R-markdown file in GitHub) the substitution bias across individual codons was the most significant predictor of the abundances of individual resistance mutations across all patients ($p=3.3e-5$ for substitution bias vs $p=0.016$ for IC_{50}). Notably, a regression model that included only growth rates in the presence and absence of drug (no substitution bias) was much less predictive (Figure 3C). To verify that our result wasn't overfit, we also identified an independent data set curated by the Sanger Institute that catalogs the abundance of different ABL1 mutations. While the mutations recorded in this data set have a less clear clinical provenance than our analysis, we decided to use them as a "test set" because they had significantly more data. The same two variables performed well in this independently generated model (Figure 3F, Supplemental Figure 2D), highlighting the significance of substitution bias as the most important predictive variable.

A stochastic, multi-mutation model of imatinib treatment predicts the prevalence of resistance mutations across ABL1.

Our experiments and epidemiology indicate that substitution probabilities that incorporate both nucleotide substitution biases and the mutational paths dictated by codon architecture are necessary to predict the distribution of specific mutations that grow out. Because of this, we wanted to know if we could predict the distribution of mutations from a mechanistic model built from first principles. We began by identifying a simple, clinically-parameterized model of CML hematopoietic stem cell division and differentiation[35]. To adapt the system to our question, we modified the model with our 19 resistance variants of interest (Figure 4A). Each mutant was parameterized with an allele-specific substitution probability (conditioned upon a resistance mutation event occurring) and drug kill term. The drug kill rates measured in our *in vitro* experiments were linearly scaled by the ratio of net growth rates of BaF3s and *in vivo* LSCs, under the assumption that the qualitative phenotype of resistance was preserved across the *in*

vitro and *in vivo* systems. We used cell-based measurements in the presence of human serum to appropriately scale drug exposures to the effective *in vivo* levels (see Methods and Supplemental Appendix 2).

Importantly, this methodology does not rely on fitting the model to the prevalence of specific resistance mutations. Therefore, it only requires a mechanistic model of treatment (i.e. birth/death rates), a list of candidate mutations (which could be generated from structure-based design or mutagenesis), measurements of mutation bias and a tractable *in vitro* system to measure the effects of putative resistance mutations.

We simulated this system of 60 differential equations stochastically (Figure 4B) for 10,000 virtual CML patients treated with imatinib (see Methods). Each patient was assigned a pharmacokinetic profile from clinically-observed distributions of *in vivo* drug concentration[36]. Similarly, patient-specific tumor detection sizes were drawn from real-world distributions[37] (See Supplemental Appendix 2). Across these 10,000 simulations, we totaled the number of *in silico* patients that relapsed with each mutation.

We conducted these simulations for a null model without substitution bias, where individual mutations were assigned the same probability, and compared its predictive value to that of a model parameterized with mutation biases. When we compared our results to previous clinical trials, we found that the total percentage of patients who acquired any resistance to imatinib was consistent with the literature in both sets of simulations (resistance incidence of 7.8% in model with mutational bias; 7.4% in model without). However, when we examined the distribution of mutations across the ABL1 kinase, a model that considered substitution biases was required to accurately predict the abundances of individual mutations (Figure 4C,D; Pearson's correlation = 0.78 vs 0.14).

A stochastic model of second-generation inhibitors predicts a decrease in the amount of drug resistance

A fundamental question in drug development is whether next-generation drugs with improved pharmacology and fewer *in vitro* resistance liabilities create better evolutionary outcomes when they are moved to the frontline. Beyond surrogate clinical endpoints, we asked whether a drug with fewer mutational liabilities can decrease the incidence of drug resistance in a population. If even imperfect drugs with clear mutational failure points can improve the outcomes of drug resistance evolution in patients, then coupling evolutionary theory to drug design could have immense practical output.

This is especially interesting because second-generation BCR-ABL inhibitors nilotinib and dasatinib have been previously evaluated in frontline clinical trials. BCR-ABL malignancies are the only indications in which the incidence of resistance mutations for first- and second-line inhibitors have been evaluated in head to head trials. Interestingly, while it has been claimed that nilotinib decreases the amount of drug resistance mutations[32], this has not been demonstrated via the use of statistical hypothesis testing. In both the ENESTnd phase 3 trial[32] for frontline nilotinib treatment and the DASISION phase 3 trial[30] for frontline dasatinib treatment, the reduction in resistance mutation frequency in the second-generation TKI arms vs imatinib control failed to reach statistical significance ($p>0.1$, chi-square test). Notably, the prevalence of resistance mutations in either arm of both trials was small (21/283 = 7.4% and 11/282 = 3.9% for imatinib and nilotinib, respectively, in the ENESTnd trial; 18/260 = 6.9% and 17/259 = 6.6% for imatinib and dasatinib, respectively, in the DASISION trial). Given the low frequency of resistance, both trials were considerably underpowered to detect a significant

difference in resistance incidence between the imatinib and second-generation TKI arms (Figure 5A). With large implications, but without sufficient data on clinical primary resistance to nilotinib or dasatinib, we turned to *in vitro* experiments and computational simulations to predict the difference in drug resistance between imatinib and second-generation TKIs.

We measured nilotinib and dasatinib IC_{50}s for the same 19 mutants and re-parameterized our treatment model (Supplemental Appendix 2 and GitHub). Then, we assessed the functional effects of protein binding upon IC_{50} measurements, allowing us to parameterize the birth and death rates across all mutants for each drug. Analysis of the entire resistance profiles of imatinib, nilotinib, and dasatinib (Figure 5B) across all 19 mutations yields the cumulative probability of any resistance-conferring mutation for each drug, a quantity we term the mutational liability. Performing simulations in an identical manner, we examined the overall proportion of patients with resistance mutations at the end of an *in silico* clinical trial. This allows us to estimate whether a second-generation drug with fewer liabilities can reduce the incidence of resistance when used in the frontline. The simulation results predict that nilotinib and dasatinib reduce the frequency of resistance relative to imatinib (Figure 5C). Notably, the reduction in resistance incidence reflects the mutational liability for each drug. Nilotinib, with a mutational liability of 0.70, yielded a 46% reduction in resistance frequency; dasatinib, with a mutational liability of 0.45, reduced resistance frequency by 54%. Thus, we predict that an appropriately powered clinical trial would be able to measure a decrease in the rate of drug resistance for both nilotinib and dasatinib.

Evolution-guided drug design could inform principled decisions between mutational vulnerabilities.

To further investigate how an evolutionarily-informed approach to drug design might affect the clinical prevalence of resistance, we imagined a hypothetical BCR-ABL TKI, which we call “maxitinib”, designed with mutational liability in mind. We simulated a cohort of *in silico* frontline CML patients for several target profiles of our hypothetical drug maxitinib; we name these distinct versions of maxitinib K1 to K15. Each of hypothetical drugs K1-K15 denote a version of maxitinib that was designed to target a different set of five of the 19 previously-discussed imatinib-resistant mutants. The top five most likely mutants are sensitive to maxitinib K1; the second through sixth most likely mutants are sensitive to maxitinib K2; and so on (Figure 5D). Except for the maxitinib-sensitive variants for each chemotype of maxitinib, drug-killing parameters for each mutant were identical to those of imatinib. Drug killing rates for maxitinib-sensitive variants matched that of wild-type BCR-ABL treated with imatinib.

The model predicts a 67% reduction in resistance incidence relative to imatinib for maxitinib K1, the hypothetical chemotype that targets the five most likely mutants (Figure 5E). The predicted resistance frequency of each maxitinib chemotype closely reflects its mutational liability.

Considerations relating to structure, conformation, and intermolecular interactions complicate drug design and likely preclude the development of a drug that targets the N most likely resistance mutants. Nevertheless, the results demonstrate the principle that second-generation drugs designed to exploit differences in the probability of resistance mutations should minimize the prevalence of resistance in a clinical population.

Discussion

Previous evolutionary theory implies (based upon predictions of pre-existing mutation probabilities) that the single fittest drug resistant variant should be selected for during drug

treatment[9,10,12,13,38,39]. However, this "survival of the fittest" principle fails to account for the extraordinary diversity in resistance mutations observed in the clinic[28–33,40,41]. In our work, we show that the probability of specific amino acid substitutions is absolutely required to predict the prevalence of imatinib-resistant mutations (Figure 3,4). We conclude that differences in substitution biases can shape the structure of intra-population heterogeneity. This structure then determines how often individual amino acid variants arise across a population. To be clear, it is inaccurate to say that drug selection is unimportant. Certainly, a variant that grows out during treatment must be drug resistant. Our analysis of CML epidemiological data (Figure 3) indicates that the degree of drug resistance conferred by a mutation is still a significant predictor of mutation prevalence. Moreover, our theoretical model (Figure 2) identifies parameter spaces where we predict natural selection will play a larger evolutionary role than substitution biases. However, in cases where heterogeneity is limited, drug resistance will prefer the path of least evolutionary resistance. In circumstances where "survival of the likeliest" is the dominant evolutionary force, the magnitude of resistance is secondary to if and when a mutation arises.

Drug resistance allows us to study parallel evolution under strong selective pressures. Previous work on adaptive parallel evolution has tended to discount the role of codon structure and biases in mutation generation in favor of natural selection[42]. In the population genetics literature, the fate of competing alleles is often referred to as clonal interference; clonal interference arguments tend to describe the outcome of evolution as time approaches infinity. At infinite time, the fittest allele will always win[43,44], and so mutation is regarded as a weak evolutionary force. In the clinic, time is not infinite. Resistance clones only appear during the limited lifetime of the pathogenic population, and once the host dies, the evolutionary experiment is over. In the case where one resistance clone has already resulted in treatment failure, the appearance of a second competing resistance clone is relatively inconsequential.

Some studies[45–47] in systems that are as diverse as phage[48] and Andean wrens[49] have begun to challenge the notion that amino acid substitution biases don't play a role in the evolutionary outcomes of traits under strong selective pressure in the real world. However, even these important prior studies have lacked the ability to quantify fitness differences in the presence of adaptive pressures (a known confounding factor)[50,51], have ignored biases due to codon usage, or have not demonstrated quantitative relationships with real world abundances[52]. Here, we can approximate these parameters in a real-world system where parallel evolution is definitely *de novo*. Our ability to use mechanistic models built on these parameters to accurately predict clinical mutational abundances strongly supports the idea that evolutionary trajectories of drug resistance can be influenced by amino acid substitution bias.

Identifying and quantifying regimes where survival of the likeliest plays a dominant evolutionary role is critical to the broad applicability of our work. Our model of a two-allele system underscores the importance of a small effective population size as a precondition for survival of the likeliest (Figure 2). In CML, this precondition is satisfied by the tumor hierarchy, where only a small population of tumor-initiating cells can seed resistant disease. Interestingly, the opposite seems likely in EGFR+ non-small-cell lung cancers (NSCLCs) treated with erlotinib; a literature survey suggests that T790M is by far the dominant resistance mutation in NSCLCs treated with erlotinib, and exhibits dramatic resistance in experimental systems[53]. However, there are other clinically relevant situations in which effective population sizes are likely restricted, and there are other cancer types that exhibit broad distributions of acquired resistance mutations in response to targeted therapy (i.e. GastroIntestinal Stromal Tumors, GIST)[54,55]. This suggests that fitness in the presence of drug is not the sole evolutionary factor in other indications as well. Chief among the variables that could restrict the effective population size in solid tumors is spatial heterogeneity. It is well accepted that solid tumors are not well-mixed and that, because of

physical and biological microenvironmental factors, only a portion of the population is mitotically active (Figure 6A). Only this actively dividing fraction of the tumor has the potential to seed resistant clones. Moreover, many therapies are given in the adjuvant setting where tumors are debulked surgically, and the remaining (smaller) tumor burden is then dosed to prevent relapse of residual tumor cells (Figure 6B). Finally, in infectious disease, transmission bottlenecks restrict the opportunity for a resistance mutant to be passed from one infected individual to the next (Figure 6C). All the aforementioned mechanisms could favor an likelier mutant over a more resistant one.

An understanding of the biology of the disease is paramount to identifying cases where survival of the likeliest can benefit drug design. Most importantly, the effective population size and mutation rate govern the degree of heterogeneity. While an ideal drug (or drug combination) would inhibit all possible mutations, no liability-free inhibitor is currently approved for frontline use[18,22]. Structural constraints on molecular design can create biophysical zero-sum games in which the ability to gain activity against a resistance mutation in a drug target inevitably comes with an off-target effect or the loss of activity against another mutation in the target[56–58]. In the future, analyses like ours should help navigate these difficult tradeoffs by prioritizing chemical matter that targets the most likely drug resistance mutations.

In circumstances where survival of the likeliest is expected to be a dominant evolutionary force in drug resistance, an approach like the one used in this study could be implemented by drug developers to predict “must-hit” resistance variants. Thermodynamic calculations and *in vitro* mutagenesis experiments (Supplemental Figure 3) can nominate potential liabilities of drugs[27]. Mutations shown to confer resistance can then be included in a computational model that is parameterized with allele-specific substitution biases, growth rates, and drug-kill rates to predict which variants will be the most prevalent. In identifying the most likely evolutionary paths to resistance, drug developers can focus on drug candidates that reduce the overall burden of resistance by hitting the most likely mutations, and not just the most thermodynamically unfavorable ones (Figure 6D).

Our work is the first study to quantitatively predict interpatient heterogeneity with a completely mechanistic model of intratumoral heterogeneity. Our predictive accuracy in clinical data definitively shifts the paradigm in studies of drug resistance and drug design. However, our predictions are still an imperfect step forward. There is unfit variance in our statistical model of the epidemiological data, and our mechanistic model has a correlation of 0.78 with clinical data. While the accuracy of these models is surprisingly high given their simplicity, there are other variables that could explain the small amount of residual variance. The first is that the genetic background in a tumor outside of ABL1 can alter the phenotypic drug resistance. Moreover, *in vivo* niches can provide protection from drug effects and/or exposure[59,60].

In diseases with a high degree of heterogeneity, even one resistance liability in a drug design is sufficient to virtually guarantee treatment failure. This is not true when heterogeneity is limited, since it is unlikely that every point mutant will be generated in the lifetime of the pathogenic population. In these cases, the magnitude of liability can determine the likelihood of resistance arising. In this study we’ve demonstrated that mitigating mutational risk is a potentially powerful strategy in minimizing the prevalence of resistance. Identifying qualitative phenotypes is an important aspect of understanding drug vulnerabilities[27], but ultimately evolutionary dynamics dictate what grows out in the clinic and defines what the patient needs. Quantitative evolutionary modeling enables us to anticipate these needs and minimize the burden of drug resistance across the population.

Methods

Construct generation

Following recombination-based cloning into pLVX-IRES-Puro, site directed mutagenesis was utilized to make the correct mutation in BCR-ABL. Mutation identity was confirmed by Sanger sequencing.

Cell line generation

BaF3 cells were ordered from DSMZ. BaF3 cells are maintained in 1640(Sigma Aldrich) +10%FBS(Fisher)+1%Penn/Strep(Life Technologies) and 10ng/mL IL-3 (PeproTech). Lentiviral constructs were co-transfected with calcium phosphate alongside third-generation packaging vectors that were pseudotyped with VSV-G. Viral supernatant was collected at 24 hours[61]. All BCR-ABL mutations were infected at limiting MOI to achieve the lowest viral titer required to produce IL-3 independence. After selection in the absence of IL-3, we tested for puromycin resistance. An assumption of BaF3 usage is that the sensitivity or resistance seen in a BaF3 cell is a reasonable approximation of the resistance and sensitivity seen in a human leukemia. This assumption has been shown to be a reasonable approximation in numerous prior studies[19,22]. Moreover, the number and diversity of mutants that were explored in this study could not be achieved by using primary samples. The rarity of CML and the limited patients observed make the collection of primary tissue harboring all mutations essentially impossible. All engineered cell lines were sequenced in the BCR-ABL kinase domain to confirm their identity.

IC_{50} measurements

Eleven serial dilutions were performed. Imatinib, dasatinib and nilotinib were all obtained from Selleck Chem. Starting points for dilutions were 10uM, 100nM, and 1uM respectively. 3000 BaF3 cells with the indicated mutation were seeded into a 96 well plate in 150ul of RPMI 1640(Sigma Aldrich) +10%FBS(Fisher)+1%Penn/Strep(Life technologies) . After addition of the drugs, cells were left in the incubator for 72 hours. At 72 hours Cell Titer Glo (Promega) was added at 1:4. This is less than the manufacturer's instructions, because we have verified the sensitivity of the assay with this reduced protocol. Plates were read via a luminescence plate reader at 72 hours.

Serum protein shifts

HSA-AAG containing medium is RPMI 1640 growth medium with the addition of 341 mM HSA (human serum albumin, Sigma, Cat # A9511) and 1 mg/ml AAG (human a1-acid glycoprotein, Sigma, Cat # G9885). All medium is sterilized by filtration through a 0.22mm membrane. Following the formulation of HAS-AAG media, identical IC_{50} curve experiments are performed. The fold change of the IC_{50} across 3 mutants of varying affinities (M244V, E255V, and WT BCR-ABL were used).

Exome data analysis

Data from the broad ExAC consortium (http://exac.broadinstitute.org/) for ABL1 was downloaded as of 11-17-2017. Data was filtered for synonymous mutations because they are more likely to be neutral than coding changes. Raw data and processing code are available in Figure 3 in our GitHub repository:
https://github.com/pritchardlabatpsu/SurvivalOfTheLikeliest/tree/master/Figures/Figure3/Mutation%20probabilities
We tallied each of the 12 possible nucleic acid substitutions (not six) because transcription coupled repair has been shown to cause biases in the mutational spectrum of the transcribed strand, and ABL1 is widely expressed. We also compared the distribution of substitutions across ABL1 in the ExAC data to genome wide mutation biases measured in CML exomes, as well as

simple transition/transversion biases from the literature, and we did not observe significant differences.

Clinical data
Clinical data was identified from six studies and the Wellcome Trust. The Sanger Wellcome Trust download was as of 12-01-2017. (https://cancer.sanger.ac.uk/cosmic/csamples/details).

Epidemiological Analysis. See Supplemental R markdown files and code repository for Figure 3. Files were written in R markdown. Raw data and analysis code(.Rmd and knitted .html files) are provided on GitHub;
https://github.com/pritchardlabatpsu/SurvivalOfTheLikeliest/tree/master/Figures/Figure3

Theoretical Model: See Supplemental Appendix 1 and code repository. .m files are included under the Figure 2C folder on GitHub.
https://github.com/pritchardlabatpsu/SurvivalOfTheLikeliest/tree/master/Figures/Figure2/Figure2C

CML model: See Supplemental Appendix 2 and code repository. All raw input data, source code, and simulation outputs are available on GitHub for Figures 4 and 5. .m files, simulation outputs, and .Rmd files for imatinib are available in the Figure 4 folder;
https://github.com/pritchardlabatpsu/SurvivalOfTheLikeliest/tree/master/Figures/Figure4
The analysis of nilotinib, dasatinib and maxitinib in figure 5 can be found at GitHub;
https://github.com/pritchardlabatpsu/SurvivalOfTheLikeliest/tree/master/Figures/Figure5

References

1. Iwasa, Y., Nowak, M. A. & Michor, F. Evolution of Resistance During Clonal Expansion. doi:10.1534/genetics.105.049791
2. Hastings, I. M. The origins of antimalarial drug resistance. *Trends Parasitol.* **20,** 512–518 (2004).
3. Goldberg, D. E., Siliciano, R. F. & Jacobs Jr., W. R. Outwitting Evolution: Fighting Drug-Resistant TB, Malaria, and HIV. *Cell* **148,** 1271–1283 (2012).
4. Bonhoeffer, S., May, R. M., Shaw, G. M. & Nowak, M. A. Virus dynamics and drug therapy. *Proc. Natl. Acad. Sci.* **94,** 6971 LP-6976 (1997).
5. Bonhoeffer, S., Lipsitch, M. & Levin, B. R. Evaluating treatment protocols to prevent antibiotic resistance. *Proc. Natl. Acad. Sci.* **94,** 12106 LP-12111 (1997).
6. Pritchard, J. R., Lauffenburger, D. A. & Hemann, M. T. Understanding resistance to combination chemotherapy. *Drug Resistance Updates* **15,** 249–257 (2012).
7. Pritchard, J. R. *et al.* Defining principles of combination drug mechanisms of action. *Proc. Natl. Acad. Sci.* **110,** E170–E179 (2013).
8. Michor, F. *et al.* Dynamics of chronic myeloid leukaemia. *Nature* **435,** 1267–1270 (2005).
9. Komarova, N. L. & Wodarz, D. Drug resistance in cancer: Principles of emergence and prevention. *Proc. Natl. Acad. Sci. U. S. A.* **102,** 9714 LP-9719 (2005).
10. Bozic, I. *et al.* Evolutionary dynamics of cancer in response to targeted combination therapy. *Elife* **2013,** (2013).
11. Goldie, J. H. & Coldman, A. J. The Genetic Origin of Drug Resistance in Neoplasms : Implications for Systemic Therapy The Genetic Origin of Drug Resistance in Neoplasms : Implications for. *Cancer Res.* **44,** 3643–3653 (1984).
12. Coldman, A. J. & Goldie, J. H. A model for the resistance of tumor cells to cancer chemotherapeutic agents. *Math. Biosci.* **65,** 291–307 (1983).

13. Komarova, N. Stochastic modeling of drug resistance in cancer. *J. Theor. Biol.* **239,** 351–366 (2006).
14. Schmitt, M. W. *et al.* Single-Molecule Sequencing Reveals Patterns of Preexisting Drug Resistance That Suggest Treatment Strategies in Philadelphia-Positive Leukemias. *Clin. Cancer Res.* (2018).
15. Picot, S. *et al.* A systematic review and meta-analysis of evidence for correlation between molecular markers of parasite resistance and treatment outcome in falciparum malaria. *Malar. J.* **8,** 89 (2009).
16. Kobayashi, S. *et al.* EGFR Mutation and Resistance of Non–Small-Cell Lung Cancer to Gefitinib. *N. Engl. J. Med.* **352,** 786–792 (2005).
17. Prediction of Susceptibility to First-Line Tuberculosis Drugs by DNA Sequencing. *N. Engl. J. Med.* **379,** 1403–1415 (2018).
18. Jabbour, E., Kantarjian, H. & Cortes, J. Use of second- and third-generation tyrosine kinase inhibitors in the treatment of chronic myeloid leukemia: an evolving treatment paradigm. *Clin. Lymphoma. Myeloma Leuk.* **15,** 323–34 (2015).
19. O'Hare, T. *et al.* AP24534, a Pan-BCR-ABL Inhibitor for Chronic Myeloid Leukemia, Potently Inhibits the T315I Mutant and Overcomes Mutation-Based Resistance. *Cancer Cell* **16,** 401–412 (2009).
20. Peters, S. *et al.* Alectinib versus Crizotinib in Untreated ALK-Positive Non-Small-Cell Lung Cancer. *N. Engl. J. Med.* NEJMoa1704795 (2017). doi:10.1056/NEJMoa1704795
21. Mok, T. S. *et al.* Osimertinib or Platinum-Pemetrexed in EGFR T790M-Positive Lung Cancer. *N. Engl. J. Med.* **376,** 629–640 (2017).
22. Wylie, A. A. *et al.* The allosteric inhibitor ABL001 enables dual targeting of BCR–ABL1. *Nature* **543,** 733–737 (2017).
23. Evans, E. K. *et al.* A precision therapy against cancers driven by KIT/PDGFRA mutations. *Sci. Transl. Med.* **9,** eaao1690 (2017).
24. Zhang, S. *et al.* The Potent ALK Inhibitor Brigatinib (AP26113) Overcomes Mechanisms of Resistance to First- and Second-Generation ALK Inhibitors in Preclinical Models. *Clin. Cancer Res.* **22,** 5527–5538 (2016).
25. Butterworth, S., Cross, D. A. E., Finlay, M. R. V., Ward, R. A. & Waring, M. J. The structure-guided discovery of osimertinib: the first U.S. FDA approved mutant selective inhibitor of EGFR T790M. *Medchemcomm* **8,** 820–822 (2017).
26. Menichincheri, M. *et al.* Discovery of Entrectinib: A New 3-Aminoindazole As a Potent Anaplastic Lymphoma Kinase (ALK), c-ros Oncogene 1 Kinase (ROS1), and Pan-Tropomyosin Receptor Kinases (Pan-TRKs) inhibitor. *J. Med. Chem.* **59,** 3392–3408 (2016).
27. Hauser, K. *et al.* Predicting resistance of clinical Abl mutations to targeted kinase inhibitors using alchemical free-energy calculations. *Commun. Biol.* **1,** 70 (2018).
28. Cortes, J. *et al.* Dynamics of BCR-ABL kinase domain mutations in chronic myeloid leukemia after sequential treatment with multiple tyrosine kinase inhibitors. *Blood* **110,** 4005 LP-4011 (2007).
29. Kim, S.-H. *et al.* Analysis of Bcr-Abl kinase domain mutations in Korean chronic myeloid leukaemia patients: poor clinical outcome of P-loop and T315I mutation is disease phase dependent. *Hematol. Oncol.* **27,** 190–197 (2009).
30. Hughes, T. P. *et al.* BCR-ABL1 mutation development during first-line treatment with dasatinib or imatinib for chronic myeloid leukemia in chronic phase. *Leukemia* **29,** 1832–1838 (2015).
31. Branford, S. *et al.* Detection of BCR-ABL mutations in patients with CML treated with imatinib is virtually always accompanied by clinical resistance, and mutations in the ATP phosphate-binding loop (P-loop) are associated with a poor prognosis. *Blood* **102,** 276 LP-283 (2003).

32. Hochhaus, A. *et al.* Nilotinib is associated with a reduced incidence of BCR-ABL mutations vs imatinib in patients with newly diagnosed chronic myeloid leukemia in chronic phase. *Blood* **121,** 3703–3708 (2013).
33. Bengió, R. M. *et al.* Clinical outcome of chronic myeloid leukemia imatinib-resistant patients: do BCR–ABL kinase domain mutations affect patient survival? First multicenter Argentinean study. *Leuk. Lymphoma* **52,** 1720–1726 (2011).
34. Ben-David, U. *et al.* Genetic and transcriptional evolution alters cancer cell line drug response. *Nature* **560,** 325–330 (2018).
35. Fassoni, A. C., Baldow, C., Roeder, I. & Glauche, I. Reduced tyrosine kinase inhibitor dose is predicted to be as effective as standard dose in chronic myeloid leukemia: a simulation study based on phase III trial data. *Haematologica* **103,** 1825–1834 (2018).
36. Peng, B., Lloyd, P. & Schran, H. Clinical Pharmacokinetics of Imatinib. *Clin. Pharmacokinet.* **44,** 879–894 (2005).
37. Stein, A. M. *et al.* BCR-ABL transcript dynamics support the hypothesis that leukemic stem cells are reduced during imatinib teatment. *Clin. Cancer Res.* **17,** 6812–6821 (2011).
38. Goldie, J. H. & Coldman, A. J. A mathematic model for relating the drug sensitivity of tumors to their spontaneous mutation rate. *Cancer Treat. Rep.* **63,** 1727–33 (1979).
39. Goldie, J. H. & Coldman, A. J. The Genetic Origin of Drug Resistance in Neoplasms: Implications for Systemic Therapy. *Cancer Res.* **44,** 3643–3653 (1984).
40. Sorbo, M. C. *et al.* Hepatitis C virus drug resistance associated substitutions and their clinical relevance: Update 2018. *Drug Resist. Updat.* **37,** 17–39 (2018).
41. Wright, A. *et al.* Epidemiology of antituberculosis drug resistance 2002–07: an updated analysis of the Global Project on Anti-Tuberculosis Drug Resistance Surveillance. *Lancet* **373,** 1861–1873 (2009).
42. Gilbert, S. F., Opitz, J. M. & Raff, R. A. Resynthesizing Evolutionary and Developmental Biology. *Dev. Biol.* **173,** 357–372 (1996).
43. Park, S.-C. & Krug, J. *Clonal interference in large populations*. (2007).
44. Gerrish, P. J. & Lenski, R. E. *The fate of competing beneficial mutations in an asexual population*. *Genetica* **102,** (1998).
45. Yampolsky, L. Y. & Stoltzfus, A. Bias in the introduction of variation as an orienting factor in evolution. *Evol. Dev.* **3,** 73–83
46. Stoltzfus, A. & McCandlish, D. M. Mutation-biased adaptation in Andean house wrens. *Proc. Natl. Acad. Sci.* **112,** 13753–13754 (2015).
47. Stoltzfus, A. & Yampolsky, L. Y. Climbing Mount Probable: Mutation as a Cause of Nonrandomness in Evolution. *J. Hered.* **100,** 637–647 (2009).
48. Rokyta, D. R., Joyce, P., Caudle, S. B. & Wichman, H. A. An empirical test of the mutational landscape model of adaptation using a single-stranded DNA virus. *Nat. Genet.* **37,** 441 (2005).
49. Galen, S. C. *et al.* Contribution of a mutational hot spot to hemoglobin adaptation in high-altitude Andean house wrens. *Proc. Natl. Acad. Sci.* **112,** 13958–13963 (2015).
50. Stoltzfus, A. & McCandlish, D. M. Mutational Biases Influence Parallel Adaptation. *Mol. Biol. Evol.* **34,** 2163–2172 (2017).
51. Lyons, D. M. & Lauring, A. S. Evidence for the Selective Basis of Transition-to-Transversion Substitution Bias in Two RNA Viruses. *Mol. Biol. Evol.* **34,** 3205–3215 (2017).
52. Powdrill, M. H. *et al.* Contribution of a mutational bias in hepatitis C virus replication to the genetic barrier in the development of drug resistance. *Proc. Natl. Acad. Sci.* **108,** 20509 LP-20513 (2011).
53. Westover, D., Zugazagoitia, J., Cho, B. C., Lovly, C. M. & Paz-Ares, L. Mechanisms of acquired resistance to first- and second-generation EGFR tyrosine kinase inhibitors. *Ann.*

Oncol. **29,** i10–i19 (2018).

54. Heinrich, M. C. *et al.* Kinase mutations and imatinib response in patients with metastatic gastrointestinal stromal tumor. *J. Clin. Oncol.* **21,** 4342–4349 (2003).
55. Wardelmann, E. *et al.* Polyclonal Evolution of Multiple Secondary KIT Mutations in Gastrointestinal Stromal Tumors under Treatment with Imatinib Mesylate. *Clin. Cancer Res.* **12,** 1743 LP-1749 (2006).
56. Wrenbeck, E., Klesmith, J., Stapleton, J. & Whitehead, T. Nicking Mutagenesis: comprehensive single-site saturation mutagenesis. *Protoc. Exch.* 1–8 (2016). doi:10.1038/protex.2016.061
57. Anastassiadis, T., Deacon, S. W., Devarajan, K., Ma, H. & Peterson, J. R. Comprehensive assay of kinase catalytic activity reveals features of kinase inhibitor selectivity. *Nat. Biotechnol.* **29,** 1039–1045 (2011).
58. Huggins, D. J., Sherman, W. & Tidor, B. Rational Approaches to Improving Selectivity in Drug Design. *J. Med. Chem.* **55,** 1424–1444 (2012).
59. Pritchard, J. R. *et al.* Bcl-2 Family Genetic Profiling Reveals Microenvironment-Specific Determinants of Chemotherapeutic Response. *Cancer Res.* **71,** 5850–5858 (2011).
60. Marusyk, A. *et al.* Non-cell-autonomous driving of tumour growth supports sub-clonal heterogeneity. *Nature* **514,** 54–8 (2014).
61. Gozgit, J. M. *et al.* RET fusions observed in lung and colorectal cancers are sensitive to ponatinib. *Oncotarget* **9,** 29654–29664 (2018).
62. Bradeen, H. A. *et al.* Comparison of imatinib mesylate, dasatinib (BMS-354825), and nilotinib (AMN107) in an N-ethyl-N-nitrosourea (ENU)-based mutagenesis screen: High efficacy of drug combinations. *Blood* **108,** 2332–2338 (2006).

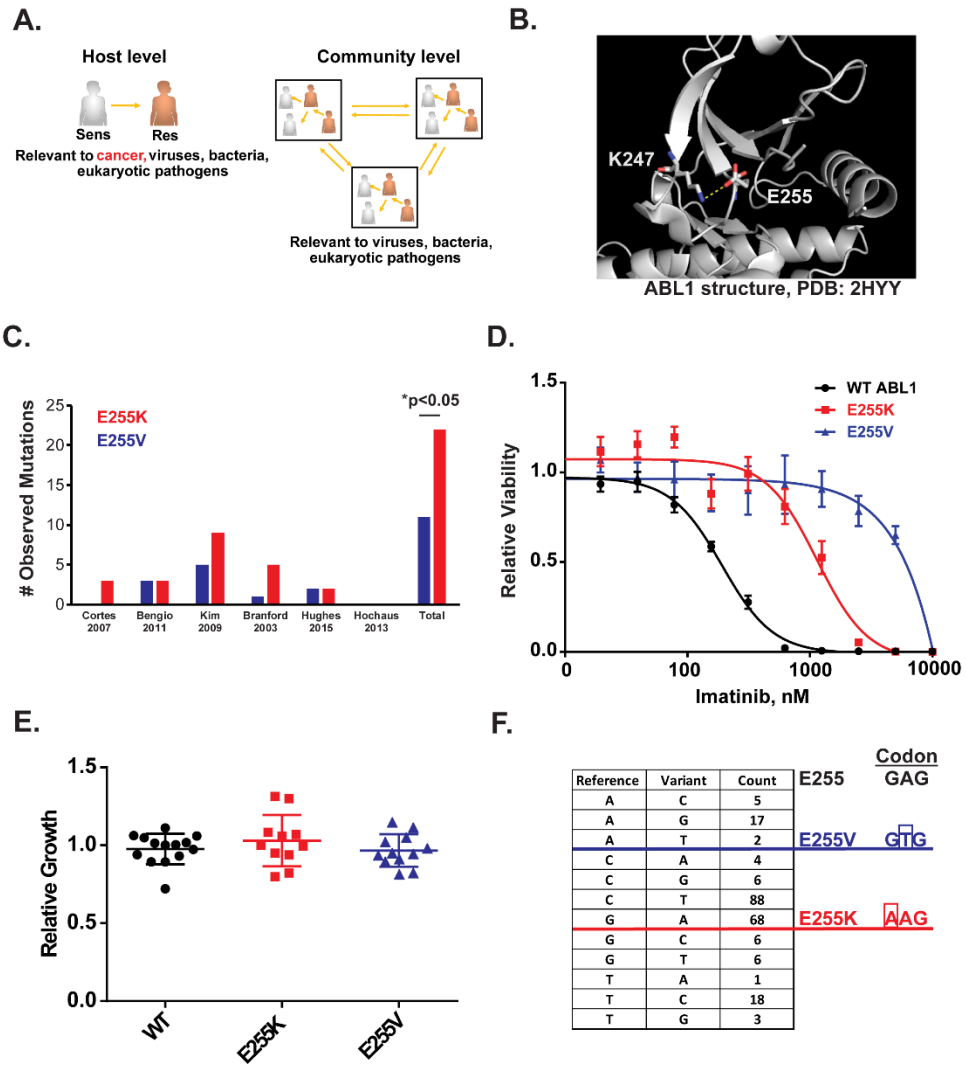

Reference	Variant	Count
A	C	5
A	G	17
A	T	2
C	A	4
C	G	6
C	T	88
G	A	68
G	C	6
G	T	6
T	A	1
T	C	18
T	G	3

Figure 1: A salt bridge in ABL1 suggests that clinical abundance may not be predicted by the amount of drug resistance conferred.
(A) A schematic of factors affecting the evolutionary dynamics of drug resistance. Without transmission, intra-tumoral variables are the only factors involved in cancer evolutionary dynamics and are limited to the host level. **(B)** ABL1 crystal structure. Ribbon diagram of secondary structure is shown. Image is zoomed in on the kinase P-loop. Loss of the E225-K247 salt bridge is associated with imatinib resistance. **(C)** Prevalence of E255K/V mutations in 6 imatinib clinical trials. A cross-trial sum is included, p-val is for chi-square test. **(D)** Imatinib IC_{50} curves for BCR-ABL transformed BaF3 cells. Relative viability is measured by Cell-Titer Glo relative to a DMSO control. N=3 per concentration, error bars are standard deviations. **(E)** Relative growth rates of BCR-ABL BaF3 variants. Each dot is an independent transduction and selection. N=11-14, error bars are standard deviations. **(F)** Substitution-specific counts of synonymous mutations in ABL1 from the Broad Institute ExAC data and the codon structure of E255. Indicated codons highlight the mutational path.

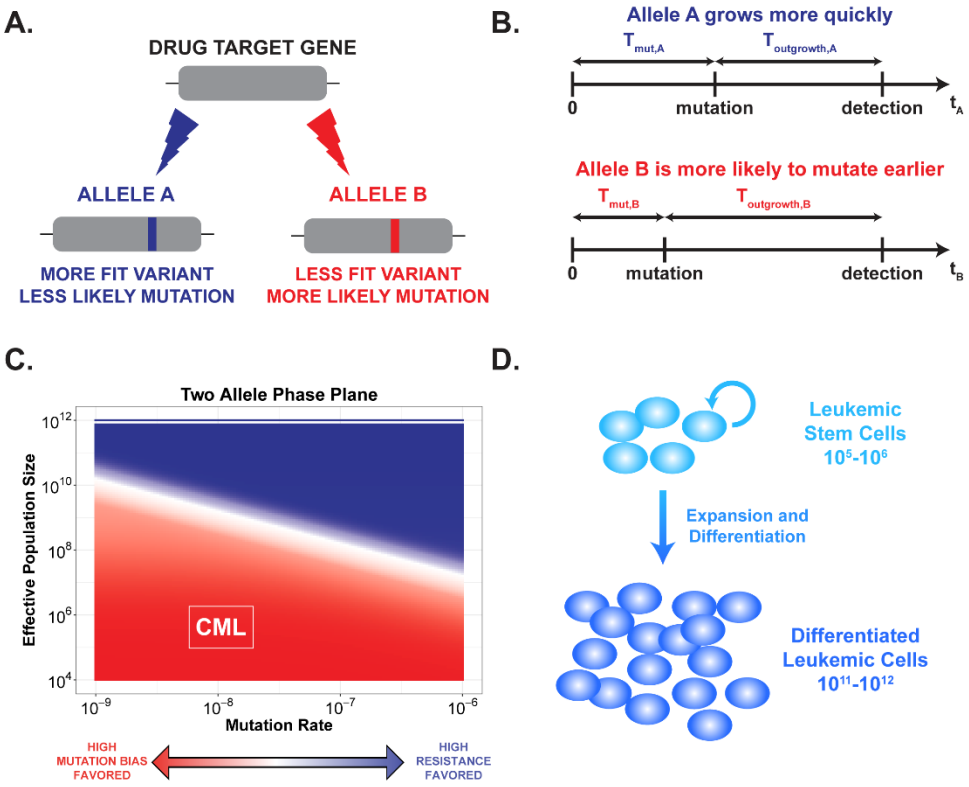

Figure 2: An analytical model of stochastic dynamics identifies where survival of the likeliest can occur.

(A) In a theoretical drug target gene with two potential resistance alleles, Allele A is assigned a high fitness and low probability, Allele B is assigned a low fitness and high probability. **(B)** A schematic of a general timeline for mutation and outgrowth for either allele given the assigned evolutionary profiles. In cases where both mutations occur, the first resistant clone to reach detection drives relapse. **(C)** A phase plane that is modeled across many mutation rates and effective population sizes. Color indicates whether Allele A (**dark blue**) or Allele B (**red**) is more likely to drive relapse. In regions where Allele B is more dominant, we expect mutation bias to be a primary evolutionary force. **(D)** Schematic of general leukemic cell population hierarchy. Only mutations in leukemic stem cells can form stable resistance clones, effectively limiting the population size to 10^5-10^6.

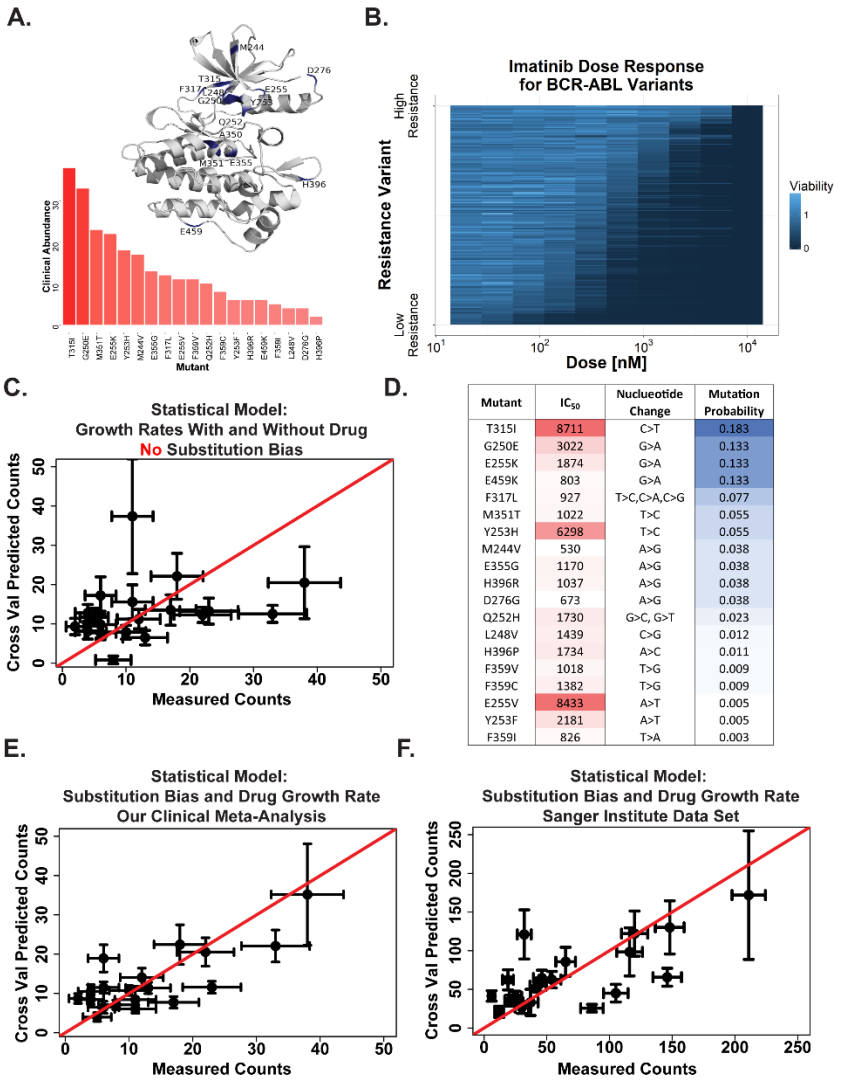

Mutant	IC_{50}	Nucleotide Change	Mutation Probability
T315I	8711	C>T	0.183
G250E	3022	G>A	0.133
E255K	1874	G>A	0.133
E459K	803	G>A	0.133
F317L	927	T>C,C>A,C>G	0.077
M351T	1022	T>C	0.055
Y253H	6298	T>C	0.055
M244V	530	A>G	0.038
E355G	1170	A>G	0.038
H396R	1037	A>G	0.038
D276G	673	A>G	0.038
Q252H	1730	G>C, G>T	0.023
L248V	1439	C>G	0.012
H396P	1734	A>C	0.011
F359V	1018	T>G	0.009
F359C	1382	T>G	0.009
E255V	8433	A>T	0.005
Y253F	2181	A>T	0.005
F359I	826	T>A	0.003

Figure 3: An analysis of epidemiologic incidences of BCR-ABL mutations.

(A) A crystal structure ribbon diagram of the ABL1 kinase domain and distribution of the 19 most prevalent BCR-ABL resistance mutants. These 19 variants account for approximately 95% of resistance mutations observed clinically in the six studies from Figure 1C. **(B)** Drug-dose response was measured by Cell-Titer Glo and is plotted in the heatmap. N=3 independent infections for all 20 cell lines (WT and mutants). The range of drug resistance conferred by these mutations is plotted in the heatmap. Each BCR-ABL BaF3 line was dosed with 11 serial dilutions of imatinib in triplicate. All cell lines are ordered by sensitivity. Raw data and code are available on GitHub. **(C)** A regression model of clinical mutation prevalence based upon the growth rates in the presence and absence of imatinib only. X-error bars are 95% binomial confidence intervals of abundance counts; Y error bars are 95% CI from LOOCV in our negative binomial regression. **(D)** A table that includes IC_{50}s (in nM) fit from the data in Figure 3B. **(E)** Observed versus predicted plots for the regression model of clinical mutation prevalence (determined by our clinical meta-analysis**)** regressed against growth rate in the presence of drug and mutational probability (which is the final model). X-error bars are 95% binomial confidence intervals of abundance counts; Y error bars are 95% CI from LOOCV in our negative binomial regression. **(F)** Observed versus predicted plots as in **3E** for independent Sanger data set.

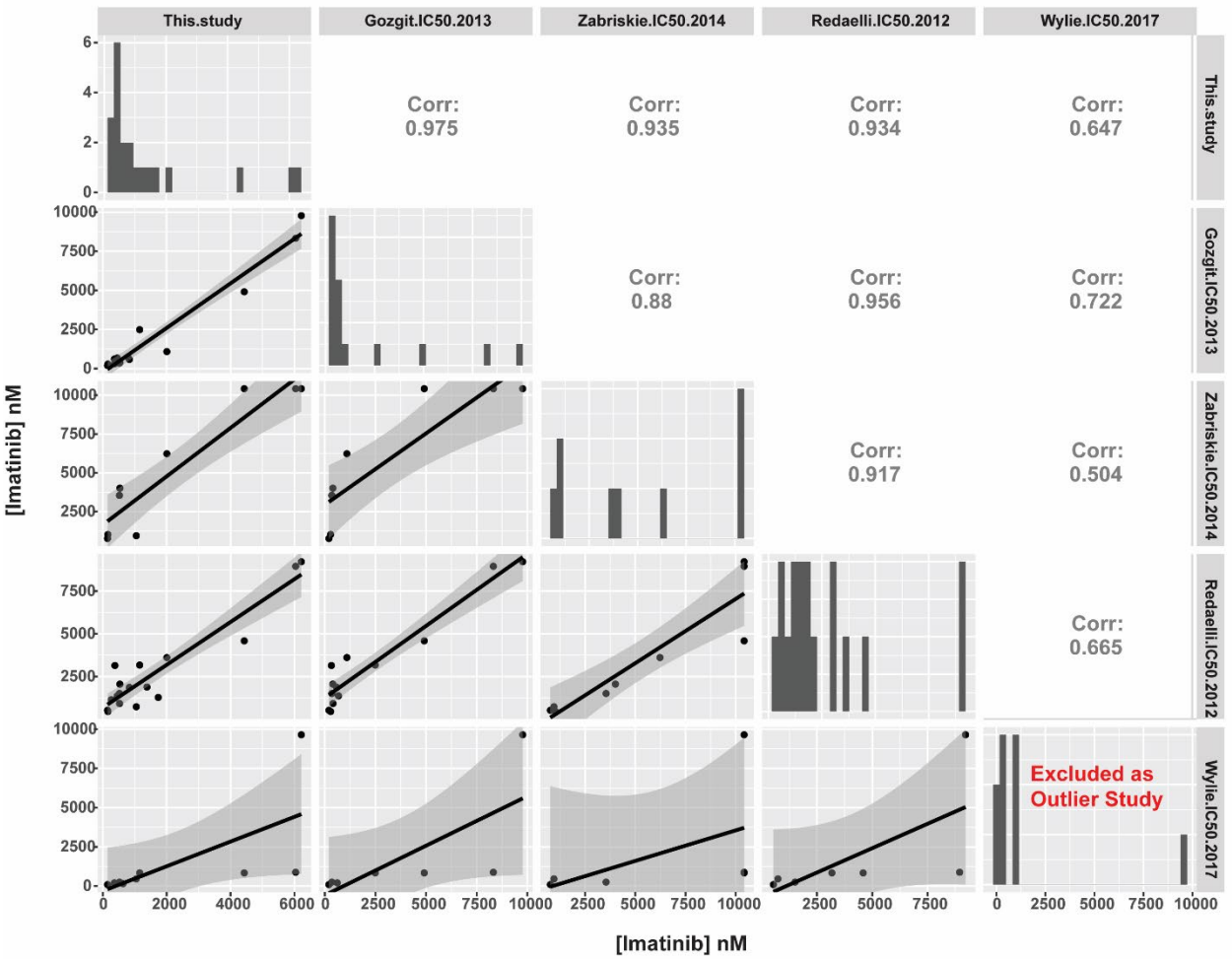

Supplemental Figure 1: Analysis of IC_{50} measurements in BCR-ABL resistance mutants across studies

We analyzed the IC_{50} of BaF3s transduced with BCR-ABL variants as reported in other studies. The diagonal of the figure shows the histogram of IC_{50}s for each study. The correlations are reported in the off-diagonals. In general, four studies (ours, Gozgit 2013, Zabriskie 2014, and Redaelli 2012) exhibit high cross-correlation (Pearson's rho ≥ 0.88). The Wylie 2017 study was excluded from further analysis given its low correlation with the remaining four studies. See Methods and Supplemental Table 1 for explanation of the normalization procedure.

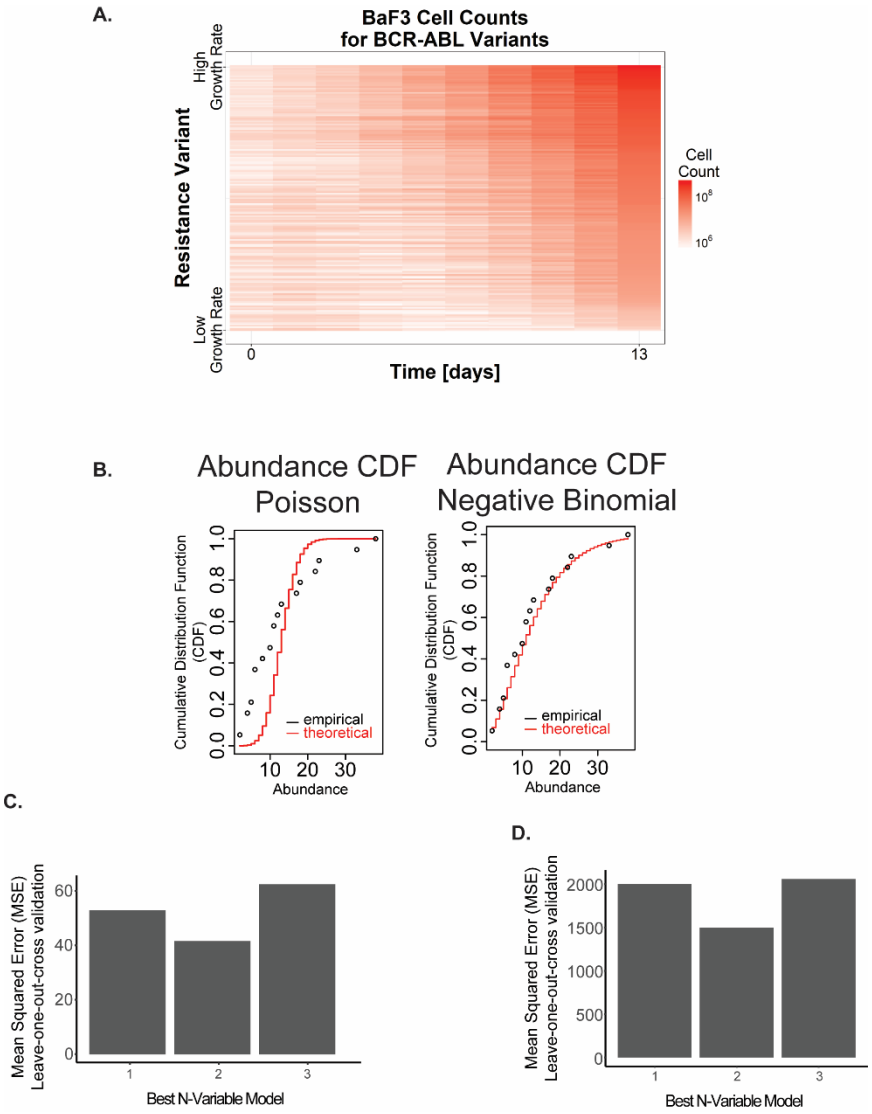

Supplemental Figure 2: Construction of resistance mutation prevalence model
A statistical model was developed to explain the variance in clinical prevalence of BCR-ABL resistance mutations. **(A)** To construct the model, we considered three potential predictor variables: imatinib IC_{50} (Figure 3B), growth rate in the absence of drug (Supplemental Figure 2A), and amino acid substitution probability (Figure 3D). **(B)** The amino acid prevalence assembled from our meta-analysis of multiple clinical trials was analyzed to identify the appropriate generalized linear model to use for regression. The empirical CDF of the prevalence count data was compared to theoretical CDFs given a Poisson (left) and negative binomial distribution (right). The Poisson distribution was overdispersed, while the negative binomial distribution appeared to agree with the empirical data and so a negative binomial regression model was used. **(C)** Validation of the regression model trained on our clinical meta-analysis data set. Leave-one-out cross validation was used to estimate the test error of the N-variable model with the lowest AIC for each N. The N=1 model includes substitution bias; the N=2 model includes substitution bias and IC_{50}; the N=3 model includes substitution bias, IC_{50}, and growth rate in the absence of drug. The N=2 model had the lowest estimated mean square error. For a complete explanation of model construction see the Figure 3 R-markdown file on GitHub. **(D)** Validation of regression model as in **(C)** for model trained on the Sanger Institute data set.

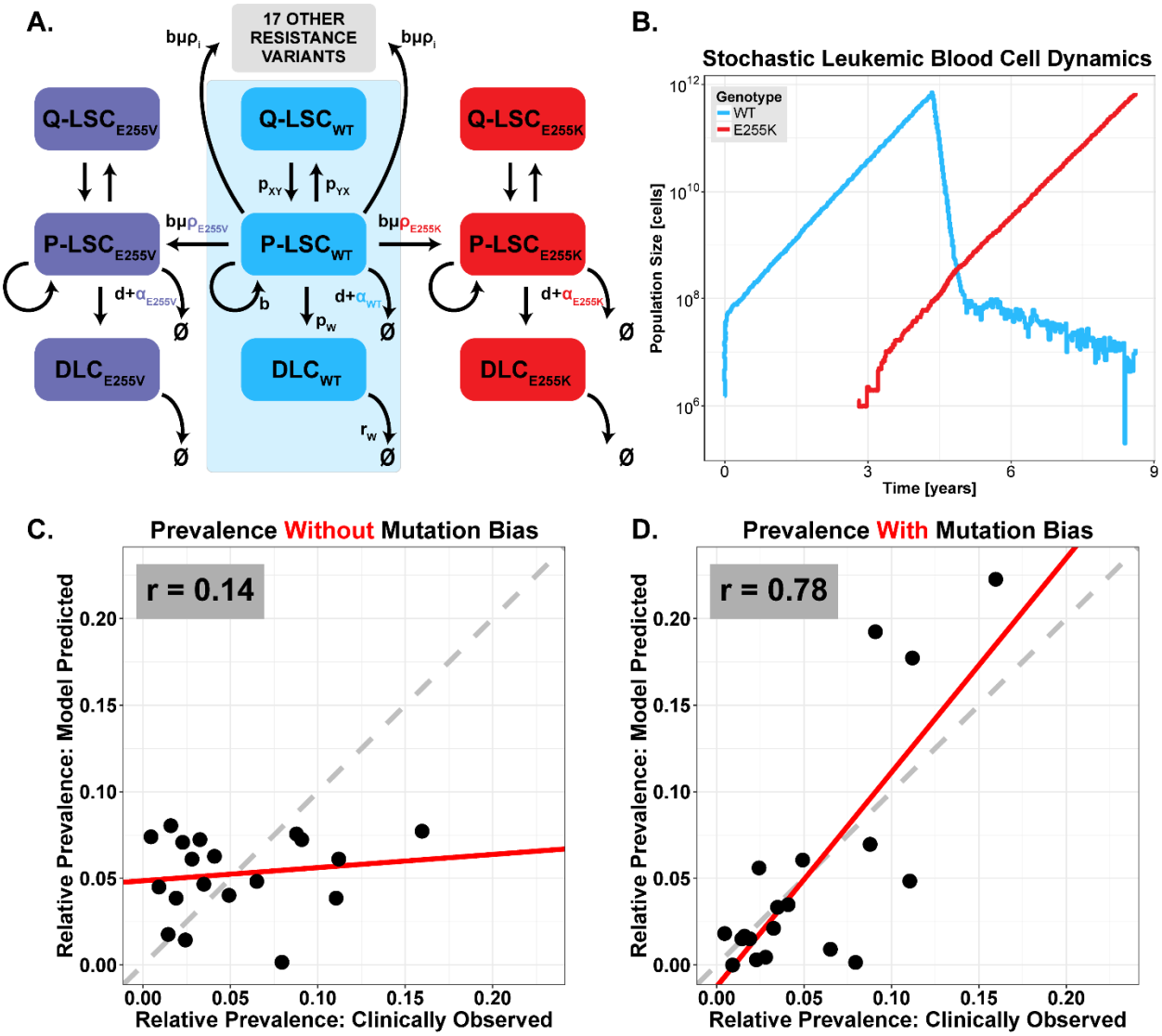

Figure 4: A mechanistic and stochastic model of CML evolutionary dynamics.

(A) Schematic of stochastic CML evolutionary dynamic model. The initial deterministic model of 3 differential equations (shaded in **blue**) is from Fassoni et al. 2018[35] and is fit to phase 3 clinical data. We reformulated a stochastic version of 60 differential equations parameterized from Fassoni et al. 2018[35] and our clinical data. Leukemic stem cells alternate between proliferating (P-LSC) and quiescent state (Q-LSC). P-LSC give rise to differentiated leukemic cells (DLC). P-LSCs may also spawn a resistant subclone P-LSC$_i$ when dividing. The allele-specific mutational probability is given by ρ_i. Note that we added the ability for all 19 resistance mutations to occur, such that there are 20 sets of differential equations with 3 populations per mutant. The system is solved stochastically. **(B)** An example stochastic simulation of the model described in **3A**. **(C)** Simulation results for the stochastic model without mutation bias (uniform ρ_i). The Pearson correlation between observed and predicted prevalences is 0.14. **(D)** Simulation results for the stochastic model with mutation bias (allele-specific ρ_i). The Pearson correlation is 0.78.

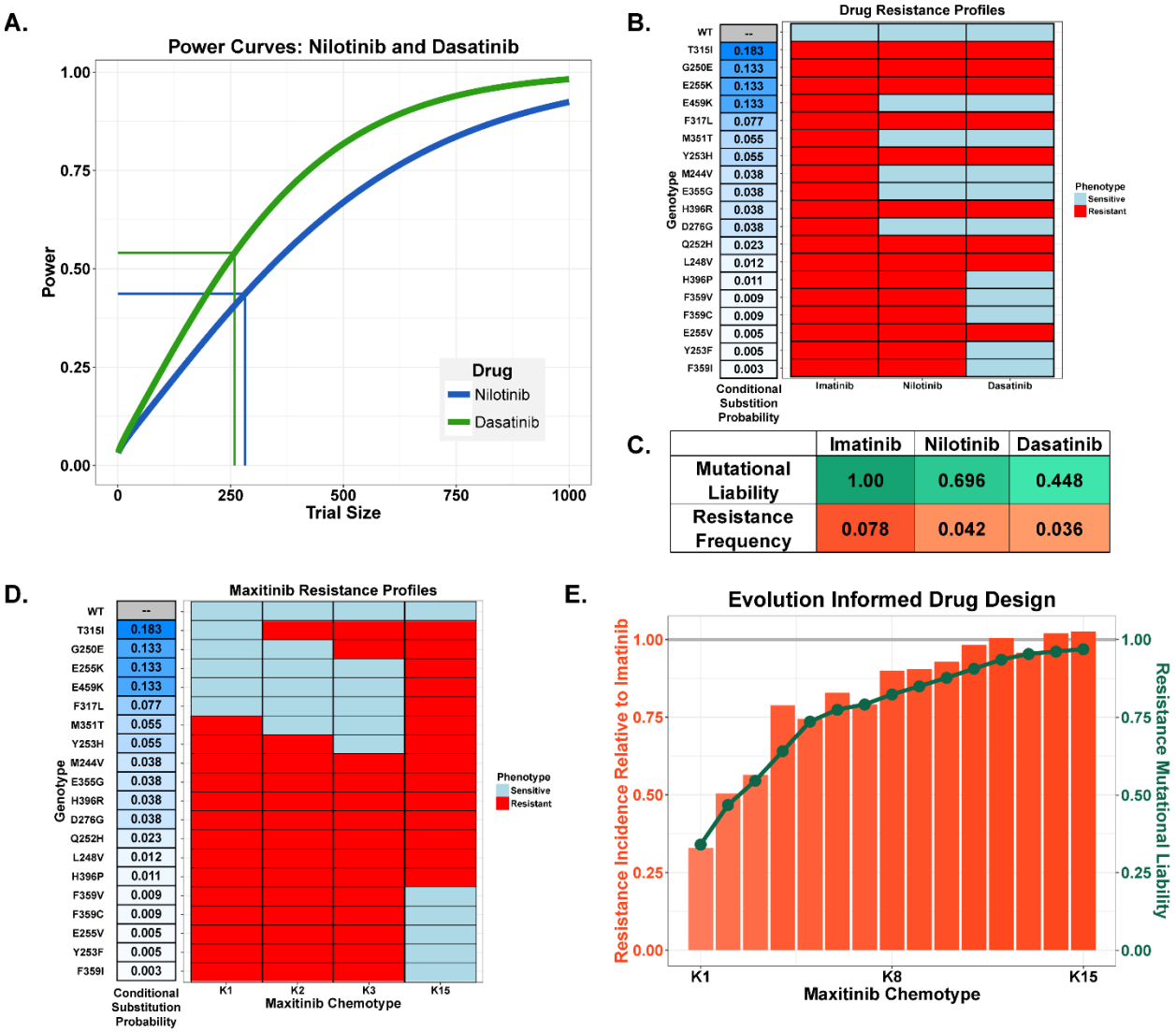

Figure 5: Drug-specific mutational liabilities and evolution guided drug design

(A) Power curves for nilotinib and dasatinib frontline clinical trials. It depicts the power to reach an alpha of 0.05 for the comparison of the total number of resistant mutants in imatinib versus the second line inhibitor. Labeled points indicate the power of the ENESTnd (frontline nilotinib; N=282 and 1-β=0.43) and DASISION (frontline dasatinib; N=259 and 1-β=0.54) phase 3 clinical trials. The assumed effect size was estimated from our simulation results. **(B)** Experimentally measured IC_{50}s create measured resistance profiles for imatinib, nilotinib, and dasatinib. **(C)** Mutational liabilities (defined as the sum of conditional probabilities of resistance-conferring mutations) and predicted resistance frequencies for imatinib, nilotinib, and dasatinib. **(D)** Resistance profiles for versions of a hypothetical drug, "maxitinib". Maxitinib K1 targets the first through fifth most likely mutants; K2 targets the second through sixth most likely; and so on. **(E)** Maxitinib simulation results. Orange bars represent the resistance incidence of each maxitinib chemotype relative to imatinib. Green points indicate mutational liability.

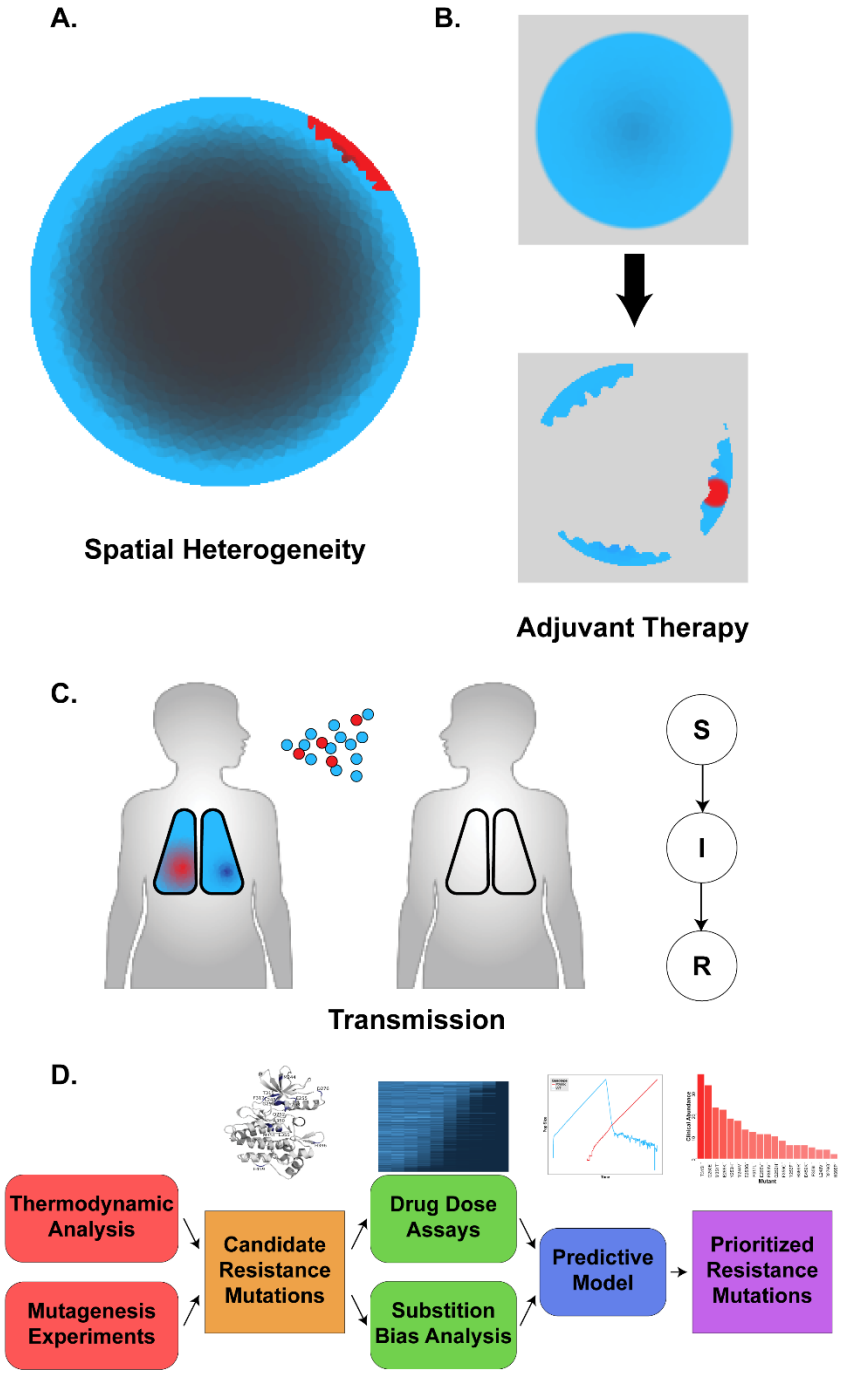

Figure 6: Cases of restricted heterogeneity where survival of the likeliest may be prominent. **(A)** A spatially heterogeneous tumor with mitotically active cells in the periphery and a quiescent/necrotic core. The effect is a reduction in the number of cells able to spawn a resistant subclone. **(B)** Adjuvant therapy involves surgically debulking the tumor, restricting the effective population size. **(C)** In infectious disease, transmission bottlenecks constrain the number (and thus heterogeneity) of pathogens passed from one host to another. **(D)** A schematic of how the process of evolutionarily guided drug design would proceed.

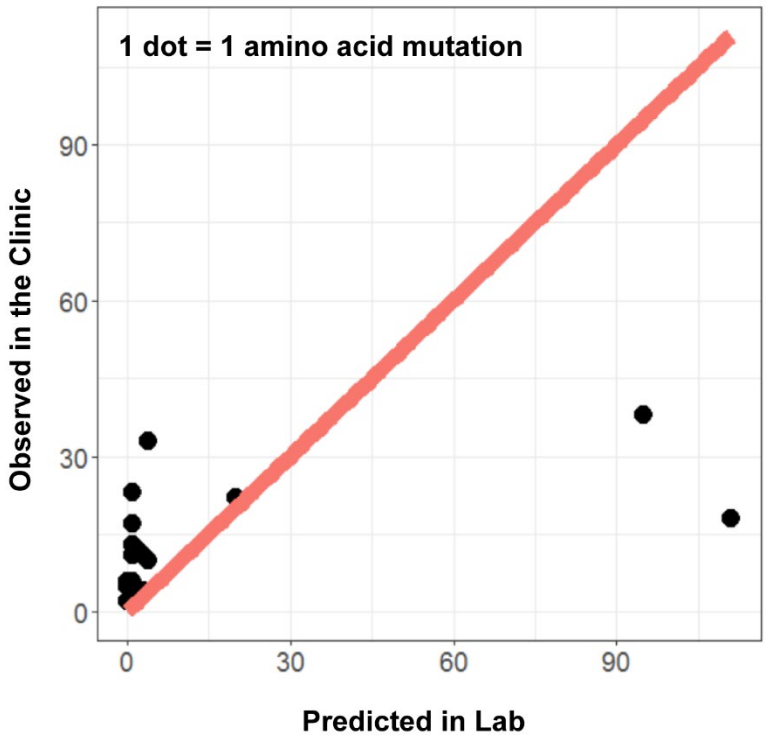

Supplemental Figure 3: ENU mutagenesis qualitatively identifies resistance mutations but fails to quantitatively predict abundance

Bradeen et al. 2006[62] have previously used ENU mutagenesis to nominate imatinib resistance mutations in BCR-ABL. The abundance of each mutation as predicted by the observation frequency in the mutagenesis experiment is given on the x-axis. The observed abundance of each mutation from our meta-analysis of clinical trials is given on the y-axis. The results indicate some qualitative concordance of resistance phenotypes between mutants predicted in the lab and those observed clinically. However, the *in vitro* mutagenesis experiment poorly predicts the quantitative frequency of mutations observed *in vivo*.